

## Accepted Manuscript

The histone methyltransferase G9a: a new therapeutic target in biliary tract cancer

Christian Mayr PhD, Katharina Helm PhD, Martin Jakab PhD, Markus Ritter MD, Rajeev Shrestha MD, Ramesh Makaju MD, Andrej Wagner MD, Martin Pichler MD, Marlena Beyreis MSc, Stefan Staettner MD, Tarkan Jaeger MD, Eckhard Klieser MD, Tobias Kiesslich PhD, Daniel Neureiter MD,MA

PII: S0046-8177(17)30409-4  
DOI: doi: [10.1016/j.humpath.2017.11.003](https://doi.org/10.1016/j.humpath.2017.11.003)  
Reference: YHUPA 4395

To appear in: *Human Pathology*

Received date: 24 August 2017  
Revised date: 31 October 2017  
Accepted date: 2 November 2017

Please cite this article as: Mayr Christian, Helm Katharina, Jakab Martin, Ritter Markus, Shrestha Rajeev, Makaju Ramesh, Wagner Andrej, Pichler Martin, Beyreis Marlena, Staettner Stefan, Jaeger Tarkan, Klieser Eckhard, Kiesslich Tobias, Neureiter Daniel, The histone methyltransferase G9a: a new therapeutic target in biliary tract cancer, *Human Pathology* (2017), doi: [10.1016/j.humpath.2017.11.003](https://doi.org/10.1016/j.humpath.2017.11.003)

This is a PDF file of an unedited manuscript that has been accepted for publication. As a service to our customers we are providing this early version of the manuscript. The manuscript will undergo copyediting, typesetting, and review of the resulting proof before it is published in its final form. Please note that during the production process errors may be discovered which could affect the content, and all legal disclaimers that apply to the journal pertain.



## The histone methyltransferase G9a: a new therapeutic target in biliary tract cancer

Christian MAYR PhD<sup>a,b,#</sup>, Katharina HELM PhD<sup>a,c,#</sup>, Martin JAKAB PhD<sup>c</sup>, Markus RITTER MD<sup>a,c,d</sup>, Rajeev SHRESTHA MD<sup>e</sup>, Ramesh MAKAJU MD<sup>f</sup>, Andrej WAGNER MD<sup>b</sup>, Martin PICHLER MD<sup>g,h</sup>, Marlena BEYREIS MSc<sup>a,c</sup>, Stefan STAETTNER MD<sup>i</sup>, Tarkan JAEGER MD<sup>j</sup>, Eckhard KLIESER MD<sup>k</sup>, Tobias KIESSLICH PhD<sup>a,b,#</sup> and Daniel NEUREITER MD, MA<sup>k,\*,#</sup>

# Equally contributed

<sup>a</sup> Laboratory for Tumour Biology and Experimental Therapies (TREAT), Institute of Physiology and Pathophysiology, Paracelsus Medical University, Strubergasse 21, 5020 Salzburg, Austria; e-mails: ch.mayr@salk.at, katharina.helm@stud.pmu.ac.at, markus.ritter@pmu.ac.at, marlena.beyreis@pmu.ac.at, t.kiesslich@salk.at

<sup>b</sup> Department of Internal Medicine I, Paracelsus Medical University / Salzburger Landeskliniken (SALK), Muellner Hauptstraße 48, 5020 Salzburg, Austria; e-mails: and.wagner@salk.at

<sup>c</sup> Laboratory of Functional and Molecular Membrane Physiology (FMMP), Institute of Physiology and Pathophysiology, Paracelsus Medical University, Strubergasse 21, 5020 Salzburg, Austria; e-mails: martin.jakab@pmu.ac.at

<sup>d</sup> Department for Radon Therapy Research, Ludwig Boltzmann Cluster for Arthritis and Rehabilitation, Institute of Physiology and Pathophysiology, Paracelsus Medical University, Strubergasse 21, 5020 Salzburg, Austria

<sup>e</sup> Cancer Research Unit, Research and Development Department, Dhulikhel Hospital, Kathmandu University, 45200 Dhulikhel, Nepal; e-mails: rmaleku@hotmail.com

<sup>f</sup> Department of Pathology, Dhulikhel Hospital, Kathmandu University Hospital, 45200 Dhulikhel, Nepal; e-mails: makajuram@yahoo.com

<sup>g</sup> Division of Oncology, Department of Internal Medicine, Medical University of Graz, Auenbruggerplatz 15, 8036 Graz, Austria; e-mails: martin.pichler@medunigraz.at

<sup>h</sup> Department of Experimental Therapeutics, The UT MD Anderson Cancer Center, 1515 Holcombe Blvd, Houston, TX 77030, USA

<sup>i</sup> Department of Visceral, Transplant and Thoracic Surgery, Medical University Innsbruck, Anichstraße 35, 6020 Innsbruck, Austria; e-mails: stefan.staettner@tirol-kliniken.at

<sup>j</sup> Department of Surgery, Paracelsus Medical University / Salzburger Landeskliniken (SALK), Muellner Hauptstraße 48, 5020 Salzburg, Austria; e-mails: ta.jaeger@salk.at

<sup>k</sup> Institute of Pathology, Paracelsus Medical University / Salzburger Landeskliniken (SALK), Muellner Hauptstraße 48, 5020 Salzburg, Austria; e-mails: e.klieser@salk.at, d.neureiter@salk.at

\* **Corresponding Author:** Assoc.-Prof. Daniel Neureiter MD, MA; Institute of Pathology, Paracelsus Medical University / Salzburger Landeskliniken (SALK), Muellner Hauptstrasse 48, 5020 Salzburg, Austria; e-mail: d.neureiter@salk.at; phone: +43 (0)5 7255-58107

**Running title:** Role of G9a in biliary tract cancer

**Conflict of interest:** none

**Funding disclosures:** This study was supported by funds of the Oesterreichische Nationalbank (Austrian Central Bank, Anniversary Fund, project number: 14842) and the research fund of the Paracelsus Medical University Salzburg (grant No. A12-02-006-KIE).

**Abstract**

The histone methyltransferase G9a (EHMT2) is a key enzyme for dimethylation of lysine 9 at histone 3 (H3K9me<sub>2</sub>), a suppressive epigenetic mark. G9a is over-expressed in tumour cells and contributes to cancer aggressiveness. Biliary tract cancer (BTC) is a rare cancer with dismal prognosis due to a lack of effective therapies. Currently, there are no data on the role of G9a in BTC carcinogenesis. We analysed G9a expression in n = 68 BTC patient specimens and correlated the data with clinico-pathological and survival data. Moreover, we measured G9a expression in a panel of BTC cell lines and evaluated the cytotoxic effect of G9a inhibition in BTC cells using established small-molecule G9a inhibitors. G9a was considerably expressed in about half of BTC cases and was significantly associated with grading and tumour size. Additionally, we observed significant differences of G9a expression between growth type and tumour localisation groups. G9a expression diametrically correlated with Vimentin (positive) and E-Cadherin (negative) expression. Importantly, survival analysis revealed G9a as a significant prognostic factor of poor survival in patients with BTC. In BTC cells, G9a and H3K9me<sub>2</sub> were detectable in a cell line-dependent manner on mRNA and/or protein level, respectively. Treatment of BTC cells with established small-molecule G9a inhibitors resulted in reduction of cell viability as well as reduced G9a and H3K9me<sub>2</sub> protein levels. The present study strongly suggests that G9a contributes to BTC carcinogenesis and may represent a potential prognostic factor as well as a therapeutic target.

**Keywords:** biliary tract cancer, epigenetics, histone methyltransferase, G9a, H3K9me<sub>2</sub>

## 1. Introduction

Epigenetic regulation is essential for cellular function and diversity. Major mechanisms include DNA methylation and histone protein modifications. Histone methylation is an epigenetic mark leading to either transcriptional activation or repression [1].

G9a (EHMT2) is a histone methyltransferase that dimethylates lysine 9 at histone 3 (H3K9me<sub>2</sub>) thus reducing transcription. G9a consists of a catalytic active SET domain, ankyrin repeats for protein-protein interactions and a nuclear localization signal [2]. Physiologically, G9a is required for correct differentiation of embryonic stem cells and immune cells [2]. G9a depletion resulted in global methylation loss specifically at euchromatin – a unique feature suggesting that G9a controls active promoter regions [2]. Overly active G9a contributes to development and progression of various cancers and is directly involved in cancer metabolism, metastasis, cell survival and response to hypoxia [2-5]. Currently, only a few studies have investigated G9a in human tumours demonstrating higher expression of G9a in cancer tissues compared to healthy controls [3, 5-10]. Moreover, high G9a expression was associated with unfavourable clinico-pathological parameters and poor survival in lung, ovarian, endometrial cancer as well as in oesophageal squamous cell and hepatocellular carcinoma (HCC) [3, 7-10].

Biliary tract cancers (BTC) are categorised into intrahepatic, perihilar, extrahepatic BTC (or cholangiocarcinoma) as well as gallbladder cancer (GBC). Although the incidence of BTC is low in developed countries (3% of gastrointestinal cancers), BTC is the second most common primary liver tumour after HCC [11]. Current therapies include surgery (applicable in only 30%), chemotherapy (cisplatin, gemcitabine), radiation, and photodynamic therapy (PDT) [11-13]. However, due to the heterogeneous and aggressive nature as well as high therapeutic resistance, prognosis remains poor with a 5-year survival rate of only 5-10% [11]. A better understanding of the molecular oncogenesis of BTC and identification of new therapeutic targets is therefore of utmost importance.

As currently no studies describe the role of G9a in BTC, this study aims at initial evaluation of G9a as a potential prognostic marker and therapeutic target in BTC and to examine the effect of G9a inhibition in an *in vitro* BTC cell model.

## 2. Materials and Methods

### 2.1 Clinical BTC samples and immunostaining

Sixty-eight (68) cases of formalin-fixed paraffin embedded (FFPE) BTC samples archived between 1997 and 2017 at the Institute of Pathology (Paracelsus Medical University, Salzburg, Austria) were included and comprise intrahepatic, perihilar and extrahepatic cases. Immunohistochemical analyses (IHC) of human BTC samples were carried out on anonymized specimens according to the local ethics committee (Reference No. 415-EP/73/37-2011). IHC for G9a (ab134062, Abcam, Cambridge, UK) was performed with a dilution of 1:200 (no pre-

treatment) as previously described for E-Cadherin and Vimentin [14] using the “quickscore” method (multiplication of the intensity [0-3] and extensity [0-100%]) [15]. For double IHC stainings, the first (G9a) and second (E-Cadherin and Vimentin) antibodies were sequentially detected with the DAB (brown colour) and Fast-Red (red) chromogen detection kit (Ventana, Tucson, USA).

## 2.2 Substances and cell culture

G9a inhibitors BIX01294 and BRD4770 were purchased from Selleckchem (Houston, USA) and dissolved in cell culture grade water (for BIX01294) or dimethyl sulfoxide (DMSO, Sigma Aldrich, Vienna, Austria; for BRD4770). UNC0642 was purchased from MedChem Express (Monmouth Junction, New Jersey, USA) and dissolved in DMSO. Inhibitors were stored in aliquot stocks of 10 mM at -20°C. Resazurin was purchased at Sigma Aldrich and dissolved in Dulbecco’s Phosphate Buffered Saline (DPBS, Sigma Aldrich).

A panel of nine cell lines was used in the experiments: BDC, CCSW-1, EGi-1, HuCCT1 [16], SkChA-1, TFK-1 as bile duct carcinoma cell lines and GBC, MzChA-1, MzChA-2 as gallbladder cancer cell lines (see [17] for references). Cells were cultured in high glucose Dulbecco’s modified Eagle’s medium (DMEM; Gibco, Life Technologies, Vienna, Austria) as described previously [17, 18]. See supplementary table 1 for cell seeding concentrations.

## 2.3 Drug Cytotoxicity

Dose-dependent cytotoxicities of BIX01294, BRD4770 and UNC0642 were tested on BTC cells grown in 96-well microplates. Cells were treated for 72 hours with various concentrations of BIX01294, BRD4770 and UNC0642 and the number of viable cells was quantified via the Resazurin assay and an Infinite M200 microplate reader (Tecan, Groedig, Austria) as described previously [17, 18]. If applicable, the 10/50/90% inhibitory concentration ( $IC_{10/50/90}$ , concentration at which number of viable cells is reduced by 10/50/90%) was calculated using linear interpolation.

## 2.4 mRNA and protein expression analysis

Total RNA was isolated with TRIzol Reagent (Ambion, Life Technologies) and the Direct-zol™ RNA MiniPrep Kit (Zymo Research, Irvine, California, USA); cDNA synthesis was done using the GoScript™ Reverse Transcription System (Promega, Mannheim, Germany). Quantification of gene expression was performed by quantitative real-time reverse transcription PCR (qRT-PCR) using GoTaq® qPCR Master Mix (Promega) on a ViiA7 real-time PCR system (Applied Biosystems, Life Technologies) according to the manufacturers’ instructions. All samples were measured in technical quadruplicates and the specificity of the primer pairs was checked via melting curve analysis. G9a expression was related to the housekeeping gene beta-actin.

Primers were purchased at Sigma Aldrich (KiCqStart® primers, sequences are available on request from the corresponding author).

For western blots, cells were seeded in 60 mm dishes until they reached 80-90% confluence and processed as described previously [17]. In short,  $10^5$  cells per sample were loaded on SDS gels (4-20% Mini-PROTEAN TGX, BioRad, Vienna, Austria) and blotted using the Trans-Blot Turbo Mini Nitrocellulose Transfer Packs System (BioRad). Membranes were incubated overnight with primary antibodies and then incubated with HRP-linked secondary antibodies as listed in supplementary table 2. After development with Signal Fire ECL Reagent (CST), protein bands were imaged using a ChemiDoc MP System (BioRad). Protein expression was quantified by calculation of grey densities using ImageJ and related to those of beta-Actin.

## 2.5 Statistics

All data points represent mean values of at least three biological replicates  $\pm$  standard error of mean. Correlation analysis was done by calculation of the Pearson's correlation coefficient. Differences in G9a expression pattern (scoring at the centre and periphery of the tumour as well as the mean value thereof) between patient samples grouped by clinico-pathological parameters were calculated using t-test and ANOVA and Bonferroni *post-hoc* test. Cut-off values for G9a IHC scores were determined for tumour periphery, centre and mean IHC scores using the receiver operating characteristic (ROC) calculation and Youden Index analysis for overall survival. Survival curves were generated using the Kaplan Meier method and compared by log rank tests (Mantel-Cox). Cox regression analysis to identify predictors of survival was performed using backward elimination Wald method for the variables localisation, grading, growth pattern, UICC staging and G9a scoring (tumour centre, periphery and mean). Statistical results were considered significant (\*) or highly significant (\*\*) at  $p < 0.05$  and  $p < 0.01$ , respectively. Calculations were done with OriginPro 2017 (OriginLab, Northampton, Massachusetts, USA) and SPSS v21 (IBM, Armonk, New York, USA).

## 3. Results

### 3.1 Clinical parameters of BTC patients

As summarised in table 1, the 68 BTC cases included  $n = 39$  [57.4%] intrahepatic,  $n = 22$  [32.4%] perihilar, and  $n = 7$  [10.2%] extrahepatic cases of BTC (aged mean 67.7, 95% CI: 65.1-70.3, range: 37.8-90.1 years). Overall survival was 22.5 months (mean, 95% CI: 15.7-29.3) and 14.8 months (median) and the tumour size was 4.1 cm (mean, 95% CI: 3.2-5.0 cm). G9a expression showed no significant difference between groups of patients classified by age, gender, TNM status, UICC and survival status.

### 3.2 G9a is expressed in BTC samples and associated with clinico-pathological data and survival

As shown in figure 1A, only 8.8% of BTC cases (6 / 68) were completely IHC-negative for G9a. Overall, G9a expression was generally more intense in the tumour periphery than in tumour centre (see inserts in figure 1A). Calculation of the cut-off value using ROC-analysis for classification into G9a high/low-expressing cases was based on IHC staining scores for each, tumour periphery, tumour centre and mean values. Classification by mean IHC values identified 7 out of 68 cases with high G9a expression, whereas the remaining 55 cases were classified as G9a low (varying IHC score). While high G9a-expressing BTC cases comprise samples with different T and UICC staging (both: 1-4), these cases are uniformly tumours of G3 differentiation.

Comparison of G9a mean expression levels between groups of different clinico-pathological characteristics (table 1 and figure 1B) indicated a significantly higher G9a expression in intrahepatic versus perihilar localisation. Moreover, G9a was more intensively expressed in mass-forming than in periductal BTC cases. Importantly, we observed a highly significant increase of G9a expression in G3 versus G2 tumours ( $p < 0.001$ ). In cases of G3 tumours with a histologically detectable G2 sub-area ( $n=6$  out of 22; exclusively in the tumour centre) the G9a expression in sub-areas with G2 differentiation (IHC scores 5 to 15) was comparable to G2-only tumours and was by trend lower than in the G3 tumour area (especially in tumour periphery).

Figure 1C summarises the correlation analysis of G9a expression (tumour centre, periphery, and mean) and tumour size as well as markers of epithelial-to-mesenchymal transition (EMT). Central, peripheral and mean G9a expression significantly positively correlated with tumour size. Regarding markers of EMT, independent of the analysed tumour area (centre, periphery or mean), we found a highly significant negative association of G9a with E-Cadherin and a highly significant positive correlation with Vimentin expression (figure 1C).

In order to evaluate G9a as a prognostic factor for overall survival, we performed Kaplan-Meier survival analysis using the cut-off values (ROC analysis) for classification of high/low G9a-expressing cases. High UICC classification, as expected, identified patients with the shortest survival ( $p = 0.016$ , figure 1D). As shown in figures 1E/F, high G9a expression was similarly associated with significantly shorter overall survival. In detail, regarding G9a expression in the tumour centre, median survival was 66.87 months for G9a low and 13.71 months for G9a high cases ( $p = 0.038$ ). Similarly, for G9a IHC mean (and tumour periphery), median survival was 66.87 months for G9a low and 13.71 months for G9a high ( $p = 0.007$ ).

Cox-regression analysis with backward Wald-method revealed a significant model ( $\chi^2 = 8.634$ ,  $p = 0.013$  after 6<sup>th</sup> step) with UICC ( $p = 0.019$ ) and G9a expression (at the tumour periphery) ( $p = 0.073$ ) as independent prognostic factors in BTC.

Representative IHC and corresponding H&E morphology images (figure 2) illustrate significantly higher G9a protein expression in intrahepatic, mass-forming and grade G3 cases compared to perihilar, periductal and G2 BTC samples, respectively (as quantified in figure

1B). In addition, spindle-cell morphology of BTC is associated with higher G9a protein expression. IHC double stainings for G9a and E-Cadherin or Vimentin are shown in figure 3 illustrating the indirect / direct association of G9a and E-Cadherin / Vimentin, respectively.

### 3.3 G9a is expressed in BTC cell lines

As illustrated in figure 4A, G9a mRNA was expressed in all tested BTC cell lines to various extents. Likewise, protein levels of G9a and H3K9me2 were detectable in all cell lines (figure 4B/C). Comparable to the mRNA levels, EGi-1 cells showed the highest protein expression (for both, G9a and H3K9me2), whereas HuCCt-1 (for H3K9me2) and SkChA-1 (for G9a) showed low protein expression. Correlation analysis of G9a mRNA, G9a protein and H3K9me2 levels revealed significant positive correlations amongst each other (figure 4D).

### 3.4 G9a inhibition reduces BTC cell viability

The effect of G9a inhibition on cell viability in BTC cells was studied for three G9a inhibitors BIX01294 [19], BRD4770 [20] and UNC0642 [21]. Drug treatment for 72 hours reduced the number of viable cells in a concentration- and cell line-dependent manner (figure 5A-C; for statistical comparison see supplementary table 3). Of note, the cytotoxic effect of BRD4770 was most dependent on the cell line and was generally weaker compared to BIX01294 and UNC0642. For BIX01294 and UNC0642, higher concentrations led to drastic reduction of BTC viability, where BIX01294 showed the overall strongest cytotoxicity as indicated by consistently low IC<sub>50</sub> values compared to the other inhibitors (figure 5D).

Correlation analysis (figure 5E) of IC<sub>50</sub> values of the three inhibitors among themselves as well as with G9a mRNA and G9a protein levels revealed a non-significant negative correlation between G9a mRNA/protein and BIX01294-IC<sub>50</sub> and UNC0642-IC<sub>50</sub>, respectively. Interestingly, we saw a highly significant correlation between BIX01294-IC<sub>50</sub> and UNC0642-IC<sub>50</sub>. Due to the weak cytotoxic effect of BRD4770 for some of the tested BTC cell lines, calculation of IC<sub>50</sub> was only possible for five of the nine cell lines (excluded from analysis).

### 3.5 G9a inhibition reduces G9a and H3K9me2 protein levels in BTC cells *in vitro*

Finally, we tested the effect of the most frequently used G9a inhibitor BIX01294 [4, 6, 22-26] on G9a, H3K9me2, E-Cadherin and Vimentin expression in CCSW-1 and EGi-1 cells (based on their G9a as well as Vimentin/E-Cadherin [14] expression characteristics). With three different BIX01294 concentrations (IC<sub>10</sub>, IC<sub>50</sub>, IC<sub>90</sub>) we observed a clear reduction of G9a and H3K9me2 protein levels in a concentration-dependent manner in both cell lines. In CCSW-1 cells, E-Cadherin was reduced in a concentration-dependent manner; however, in CCSW-1 cells, basal E-Cadherin levels are very low. In EGi-1 cells, treatment with IC<sub>50</sub>-BIX01294 resulted in enhanced E-Cadherin protein levels, whereas IC<sub>90</sub>-BIX01294 strongly reduced E-

Cadherin protein levels. In CCSW-1, Vimentin expression was slightly but nonetheless significantly diminished after BIX01294 treatment (Vimentin not detectable in EGi-1 cells).

#### 4. Discussion

Here, we provide first information on the relevance of histone methyltransferase G9a in BTC carcinogenesis. In accordance with previous publications regarding other cancer entities, we observed significant expression of G9a in human BTC samples [3, 5, 7-9, 27]. G9a clearly correlated with unfavourable clinico-pathological characteristics, specifically with tumour size and grading. This first description of such correlations for BTC is in line with a previous study in oesophageal squamous cell carcinoma where G9a expression was associated with histological grade and tumour stage [10]. Likewise, in HCC, G9a correlated with aggressive tumour characteristics such as TNM stage [9]. Of note, this study describes a step-wise increase of G9a from normal liver (lowest expression), over chronic hepatitis, cirrhotic liver and, finally, to early and advanced HCC, suggesting a role of G9a in HCC development and progression [9]. Interestingly, we observed a highly significant increase in G9a expression from G2 and G3-graded BTC cases. Sub-analysis of G3 tumour with a detectable G2 area showed that this G9a expression pattern is also mirrored within a given BTC case. For future studies it will be interesting to see whether an (stepwise) increase of G9a expression is observable in progression of BTC on a histological level. Importantly, G9a was a predictor of poor overall survival and an independent prognostic factor in our BTC cohort – in line with studies describing a connection between G9a expression and poor survival in lung [3], ovarian [8] and oesophageal squamous cell carcinoma [10].

EMT is a complex process involved in cancer invasion and metastasis, in which E-Cadherin serves as a negative and Vimentin as a positive effector [14, 28]. Other studies reported a significant correlation of G9a expression and formation of local and distant metastases [5, 9, 10] and that G9a directly represses E-Cadherin as a marker of (benign) epithelial cell phenotype [2, 7, 29]. Although a highly significant negative correlation between G9a and E-Cadherin exists in BTC, *in vitro* G9a inhibition using BIX01294 failed to consistently restore E-Cadherin protein levels in our study. This discrepancy may be explained by generally high cytotoxic effects of the BIX01294-IC<sub>50</sub> concentration as well as by the fact that in (artificial) 2D cell culture systems, mechanisms regulating cell attachment and extracellular matrix association might be different from the physiological situation. Additionally, several publications describe different interaction partners (DNMT1 [3, 30]) and non-histone targets (p53 [31]) of G9a, which might explain cell line- or cancer-specific regulatory mechanisms of G9a.

We recently published that another SET-domain histone methyltransferase called EZH2 is involved in BTC [18]. EZH2 is the enzymatic part of the polycomb repressive complex 2 (PRC2) that specifically tri-methylates lysine 27 at histone 3 (H3K27me3), a repressive

epigenetic mark [32]. There is evidence that G9a directly coordinates PRC2 and H3K27me<sub>3</sub>, because G9a was necessary for mono-methylation of H3K27 (a prerequisite for PRC2-dependent H3K27me<sub>3</sub> [33]) and because G9a directly interacts with PRC2 [34]. Of note, this study also describes several genes directly regulated (at promoter level) by coordinated G9a and PRC2 recruitment [34]. Dual G9a and PRC2 inhibition might therefore be an interesting therapeutic strategy which also addresses the commonly observed problem that removal of H3K27me<sub>3</sub> (PRC2 inhibition) is not sufficient to reactivate PRC2-silenced genes [35]. In fact, dual inhibition of G9a and PRC2 using small-molecule inhibitors (but not single treatments) massively enhanced *spink1* target mRNA levels [35]. Therefore, subsequent studies should evaluate dual G9a and PRC2 inhibition in BTC cells and tumours.

Pharmacological G9a inhibition resulted in significant reduction of viable BTC cells in a concentration- and cell line-dependent manner. Interestingly, we found a significant correlation between BIX01294-IC<sub>50</sub> and UNC0642-IC<sub>50</sub> values in our BTC cell model – both inhibitors competitively inhibit H3K9 substrate binding [20, 21] – whereas we found no correlation of BRD4770-IC<sub>50</sub> (a S-adenosylmethionine [SAM, methyl donor] mimic [20]) with neither BIX01294-IC<sub>50</sub>, nor UNC0642-IC<sub>50</sub>. Importantly, by using different BTC cell lines and G9a inhibitors, the observed viability reduction is rather a result of actual G9a inhibition than a substance- or cell line-specific effect. However, future studies should investigate potential side- and off-target effects of these substances in an appropriate BTC *in vivo* model.

Taken together, the present study provides first data on a role of G9a in the context of biliary tract carcinogenesis by demonstrating G9a expression in human BTC samples and its association with unfavourable clinico-pathological characteristics and overall survival. Moreover, *in vitro* pharmacologic inhibition of G9a resulted in diminished G9a and H3K9me<sub>2</sub> levels with a dose-dependent reduction of viable BTC cells. Therefore, G9a might be a new diagnostic and therapeutic target for BTC. However, future studies investigating the functional role of G9a as well as potential interaction partners or non-histone targets in BTC are required.

## Acknowledgements

The expert technical assistance of Mrs Berta Lechner is gratefully acknowledged.

## Authors contributions

CM, KH, MB, TK, DN performed the research. CM, RS, RM, MR, TK, DN designed the research study. MJ, MP, SS, TJ, EK contributed essential reagents / tools / materials. CM, KH, MJ, AW, EK, MP, MB, TK, DN analysed the data. CM, KH, TK, DN wrote the paper. All authors read and approved the final version of the manuscript.

## References

1. Egger G, Liang G, Aparicio A, Jones PA. Epigenetics in human disease and prospects for epigenetic therapy. *Nature* 2004; 429:457-63.
2. Casciello F, Windloch K, Gannon F, Lee JS. Functional Role of G9a Histone Methyltransferase in Cancer. *Front Immunol* 2015; 6:487.
3. Chen MW, Hua KT, Kao HJ, Chi CC, Wei LH, Johansson G, Shiah SG, Chen PS, Jeng YM, Cheng TY, Lai TC, Chang JS, Jan YH, Chien MH, Yang CJ, Huang MS, Hsiao M, Kuo ML. H3K9 histone methyltransferase G9a promotes lung cancer invasion and metastasis by silencing the cell adhesion molecule Ep-CAM. *Cancer Res* 2010; 70:7830-40.
4. Kim Y, Kim YS, Kim DE, Lee JS, Song JH, Kim HG, Cho DH, Jeong SY, Jin DH, Jang SJ, Seol HS, Suh YA, Lee SJ, Kim CS, Koh JY, Hwang JJ. BIX-01294 induces autophagy-associated cell death via EHMT2/G9a dysfunction and intracellular reactive oxygen species production. *Autophagy* 2013; 9:2126-39.
5. Lin X, Huang Y, Zou Y, Chen X, Ma X. Depletion of G9a gene induces cell apoptosis in human gastric carcinoma. *Oncol Rep* 2016; 35:3041-9.
6. Guo AS, Huang YQ, Ma XD, Lin RS. Mechanism of G9a inhibitor BIX01294 acting on U251 glioma cells. *Mol Med Rep* 2016; 14:4613-21.
7. Hsiao SM, Chen MW, Chen CA, Chien MH, Hua KT, Hsiao M, Kuo ML, Wei LH. The H3K9 Methyltransferase G9a Represses E-cadherin and is Associated with Myometrial Invasion in Endometrial Cancer. *Ann Surg Oncol* 2015; 22 Suppl 3:S1556-65.
8. Hua KT, Wang MY, Chen MW, Wei LH, Chen CK, Ko CH, Jeng YM, Sung PL, Jan YH, Hsiao M, Kuo ML, Yen ML. The H3K9 methyltransferase G9a is a marker of aggressive ovarian cancer that promotes peritoneal metastasis. *Mol Cancer* 2014; 13:189.
9. Wei L, Chiu DK, Tsang FH, Law CT, Cheng CL, Au SL, Lee JM, Wong CC, Ng IO, Wong CM. Histone methyltransferase G9a promotes liver cancer development by epigenetic silencing of tumor suppressor gene RARRES3. *J Hepatol* 2017; 67:758-69.
10. Zhong X, Chen X, Guan X, Zhang H, Ma Y, Zhang S, Wang E, Zhang L, Han Y. Overexpression of G9a and MCM7 in oesophageal squamous cell carcinoma is associated with poor prognosis. *Histopathology* 2015; 66:192-200.
11. Razumilava N, Gores GJ. Cholangiocarcinoma. *Lancet* 2014; 383:2168-79.
12. Valle JW, Furuse J, Jitlal M, Beare S, Mizuno N, Wasan H, Bridgewater J, Okusaka T. Cisplatin and gemcitabine for advanced biliary tract cancer: a meta-analysis of two randomised trials. *Ann Oncol* 2014; 25:391-8.
13. Wagner A, Denzer UW, Neureiter D, Kiesslich T, Puespoeck A, Rauws EA, Emmanuel K, Degenhardt N, Frick U, Beuers U, Lohse AW, Berr F, Wolkersdorfer GW. Temoporfin improves efficacy of photodynamic therapy in advanced biliary tract carcinoma: A multicenter prospective phase II study. *Hepatology* 2015; 62:1456-65.

14. Urbas R, Mayr C, Klieser E, Fuereder J, Bach D, Stattner S, Primavesi F, Jaeger T, Stanzer S, Ress AL, Loffelberger M, Wagner A, Berr F, Ritter M, Pichler M, Neureiter D, Kiesslich T. Relevance of MicroRNA200 Family and MicroRNA205 for Epithelial to Mesenchymal Transition and Clinical Outcome in Biliary Tract Cancer Patients. *Int J Mol Sci* 2016; 17.
15. Detre S, Saclani Jotti G, Dowsett M. A "quickscore" method for immunohistochemical semiquantitation: validation for oestrogen receptor in breast carcinomas. *J Clin Pathol* 1995; 48:876-8.
16. Miyagiwa M, Ichida T, Tokiwa T, Sato J, Sasaki H. A new human cholangiocellular carcinoma cell line (HuCC-T1) producing carbohydrate antigen 19/9 in serum-free medium. *In Vitro Cell Dev Biol* 1989; 25:503-10.
17. Mayr C, Wagner A, Loeffelberger M, Bruckner D, Jakab M, Berr F, Di Fazio P, Ocker M, Neureiter D, Pichler M, Kiesslich T. The BMI1 inhibitor PTC-209 is a potential compound to halt cellular growth in biliary tract cancer cells. *Oncotarget* 2016; 7:745-58.
18. Mayr C, Wagner A, Stoecklinger A, Jakab M, Illig R, Berr F, Pichler M, Di Fazio P, Ocker M, Neureiter D, Kiesslich T. 3-Deazaneplanocin A May Directly Target Putative Cancer Stem Cells in Biliary Tract Cancer. *Anticancer Res* 2015; 35:4697-705.
19. Kubicek S, O'Sullivan RJ, August EM, Hickey ER, Zhang Q, Teodoro ML, Rea S, Mechtler K, Kowalski JA, Homon CA, Kelly TA, Jenuwein T. Reversal of H3K9me2 by a small-molecule inhibitor for the G9a histone methyltransferase. *Mol Cell* 2007; 25:473-81.
20. Yuan Y, Wang Q, Paulk J, Kubicek S, Kemp MM, Adams DJ, Shamji AF, Wagner BK, Schreiber SL. A small-molecule probe of the histone methyltransferase G9a induces cellular senescence in pancreatic adenocarcinoma. *ACS Chem Biol* 2012; 7:1152-7.
21. Liu F, Barsyte-Lovejoy D, Li F, Xiong Y, Korboukh V, Huang XP, Allali-Hassani A, Janzen WP, Roth BL, Frye SV, Arrowsmith CH, Brown PJ, Vedadi M, Jin J. Discovery of an in vivo chemical probe of the lysine methyltransferases G9a and GLP. *J Med Chem* 2013; 56:8931-42.
22. Pang AL, Title AC, Rennert OM. Modulation of microRNA expression in human lung cancer cells by the G9a histone methyltransferase inhibitor BIX01294. *Oncol Lett* 2014; 7:1819-25.
23. Oh SY, Seok JY, Choi YS, Lee SH, Bae JS, Lee YM. The Histone Methyltransferase Inhibitor BIX01294 Inhibits HIF-1 $\alpha$  Stability and Angiogenesis. *Mol Cells* 2015; 38:528-34.
24. Savickiene J, Treigyte G, Stirblyte I, Valiuliene G, Navakauskiene R. Euchromatic histone methyltransferase 2 inhibitor, BIX-01294, sensitizes human promyelocytic leukemia HL-60 and NB4 cells to growth inhibition and differentiation. *Leuk Res* 2014; 38:822-9.

25. Cui J, Sun W, Hao X, Wei M, Su X, Zhang Y, Su L, Liu X. EHMT2 inhibitor BIX-01294 induces apoptosis through PMAIP1-USP9X-MCL1 axis in human bladder cancer cells. *Cancer Cell Int* 2015; 15:4.
26. Ding J, Li T, Wang X, Zhao E, Choi JH, Yang L, Zha Y, Dong Z, Huang S, Asara JM, Cui H, Ding HF. The histone H3 methyltransferase G9A epigenetically activates the serine-glycine synthesis pathway to sustain cancer cell survival and proliferation. *Cell Metab* 2013; 18:896-907.
27. Huang T, Zhang P, Li W, Zhao T, Zhang Z, Chen S, Yang Y, Feng Y, Li F, Shirley Liu X, Zhang L, Jiang G, Zhang F. G9A promotes tumor cell growth and invasion by silencing CASP1 in non-small-cell lung cancer cells. *Cell Death Dis* 2017; 8:e2726.
28. Mayr C, Beyreis M, Wagner A, Pichler M, Neureiter D, Kiesslich T. Deregulated MicroRNAs in Biliary Tract Cancer: Functional Targets and Potential Biomarkers. *Biomed Res Int* 2016; 2016:4805270.
29. Dong C, Wu Y, Yao J, Wang Y, Yu Y, Rychahou PG, Evers BM, Zhou BP. G9a interacts with Snail and is critical for Snail-mediated E-cadherin repression in human breast cancer. *J Clin Invest* 2012; 122:1469-86.
30. Esteve PO, Chin HG, Smallwood A, Feehery GR, Gangisetty O, Karpf AR, Carey MF, Pradhan S. Direct interaction between DNMT1 and G9a coordinates DNA and histone methylation during replication. *Genes Dev* 2006; 20:3089-103.
31. Huang J, Dorsey J, Chuikov S, Perez-Burgos L, Zhang X, Jenuwein T, Reinberg D, Berger SL. G9a and Glp methylate lysine 373 in the tumor suppressor p53. *J Biol Chem* 2010; 285:9636-41.
32. Sauvageau M, Sauvageau G. Polycomb group proteins: multi-faceted regulators of somatic stem cells and cancer. *Cell Stem Cell* 2010; 7:299-313.
33. Wu H, Chen X, Xiong J, Li Y, Li H, Ding X, Liu S, Chen S, Gao S, Zhu B. Histone methyltransferase G9a contributes to H3K27 methylation in vivo. *Cell Res* 2011; 21:365-7.
34. Mozzetta C, Pontis J, Fritsch L, Robin P, Portoso M, Proux C, Margueron R, Ait-Si-Ali S. The histone H3 lysine 9 methyltransferases G9a and GLP regulate polycomb repressive complex 2-mediated gene silencing. *Mol Cell* 2014; 53:277-89.
35. Curry E, Green I, Chapman-Rothe N, Shamsaei E, Kandil S, Cherblanc FL, Payne L, Bell E, Ganesh T, Srimongkolpithak N, Caron J, Li F, Uren AG, Snyder JP, Vedadi M, Fuchter MJ, Brown R. Dual EZH2 and EHMT2 histone methyltransferase inhibition increases biological efficacy in breast cancer cells. *Clin Epigenetics* 2015; 7:84.

## Tables

**Table 1.** Clinico-pathological characterisation of the BTC patient cohort and G9a expression by immunohistochemistry (IHC).

		Total		mean G9a IHC score			ANOVA
		n	%	mean	stdev	95% CI	p value
	<b>All cases</b>	68	100.0	27.3	41.0	17.4-37.2	-
<b>Age (years)</b>	<60	13	19.1	37.6	47.1	9.1-66.1	0.318
	≥60	55	80.9	24.9	39.5	14.2-35.5	
<b>Gender</b>	female	28	41.2	22.2	25.4	12.4-32.1	0.398
	male	40	58.8	30.8	49.1	15.1-46.5	
<b>Tumour localisation</b>	intrahepatic	39	57.4	38.3	46.7	23.1-53.4	0.020 <sup>*, a</sup>
	perihilar	22	32.4	8.2	7.5	4.9-11.6	
	extrahepatic	7	10.3	26.1	51.7	-21.7-73.8	
<b>Growth pattern</b>	mass-forming	32	47.1	45.2	48.8	27.6-62.8	0.002 <sup>***, a</sup>
	periductal	34	50.0	11.3	23.9	2.9-19.6	
	intraductal	2	2.9	13.1	18.6	-153.6-179.9	
<b>T status (2017)</b>	T1	22	32.4	35.1	37.7	18.4-51.7	0.661
	T2	33	48.5	23.7	43.7	8.2-39.2	
	T3	10	14.7	19.0	43.6	-12.2-50.2	
	T4	3	4.4	37.5	30.7	-38.8-113.8	
<b>N status (2017)</b>	N0	36	52.9	32.3	46.9	16.5-48.2	0.367
	N1	25	36.8	25.3	36.2	10.3-40.2	
	N2	7	10.3	8.8	11.7	-2.0-19.5	
<b>M status (2017)</b>	M0	58	85.3	28.0	39.9	17.5-38.4	0.754
	M1	10	14.7	23.5	49.1	-11.6-58.6	
<b>UICC (2017)</b>	I	16	23.5	25.1	25.9	11.3-38.9	0.337
	II	18	26.5	42.2	60.5	12.1-72.3	
	III	21	30.9	21.4	24.3	10.4-32.5	
	IV	13	19.1	18.8	43.5	-7.4-45.1	
<b>Tumour grading</b>	G1	4	5.9	26.3	28.9	-19.7-72.2	<0.001 <sup>**, a</sup>
	G2	41	60.3	9.5	10.5	6.2-12.9	
	G3	22	32.4	61.4	56.4	36.3-86.4	
	G4	1	1.5	-	-	-	
<b>Survival</b>	no	30	44.1	35.5	55.4	14.8-56.2	0.144
	yes	38	55.9	20.8	23.3	13.2-28.5	

<sup>a</sup> see figure 1B for details on group comparisons.

\* indicate significant ( $p < 0.05$ ) and \*\* indicate highly significant ( $p < 0.01$ ) results

## Figure legends

### Figure 1. Expression of G9a in BTC specimens and correlation with clinico-pathological characteristics and survival data

< preferred width: single column, colour in web and print >

(A) Mean G9a expression (mean G9a IHC score) for n = 68 BTC specimens. Mean G9a IHC scores and cut-off values were calculated based on staining intensity and extensity. The inserts show the IHC scores for tumour centre (upper insert) and tumour periphery (lower insert). (B) Comparison of G9a expression for tumour localization, growth type and grading. (C) Correlation analysis of G9a (IHC expression in tumour centre, periphery, and mean), tumour size, E-Cadherin and Vimentin expression. Green boxes indicate positive, red boxes indicate negative correlation. (D-F) Survival analysis (Kaplan-Meier) of UICC classification, and G9a IHC scores at tumour centre, mean and periphery. Classification into G9a low/high expressing cases is based on ROC analysis as described in Material and Methods. \* indicate significant ( $p < 0.05$ ) and \*\* indicate highly significant ( $p < 0.01$ ) results. Abbreviations: BTC: biliary tract cancer; IHC: immunohistochemistry.

### Figure 2. Immunohistochemistry images of BTC cases.

< preferred width: double column, colour in web and print >

Representative images of H&E morphology (left) and G9a immunohistochemistry (overview and detail, right) for categories with significant differences in G9a expression. Scale bar (yellow) indicates 100 or 20  $\mu\text{m}$  for 10 x and 40 x magnification, respectively. Abbreviations: BTC: biliary tract cancer.

### Figure 3. Double-staining immunohistochemistry.

< preferred width: single column, colour in web and print >

Representative images of H&E morphology (left) and immunohistochemistry double stained for G9a (brown staining) and Vimentin (middle, red staining) or E-Cadherin (right, red staining). Scale bar (yellow) indicates 20  $\mu\text{m}$  (40 x magnification).

### Figure 4. Expression of G9a in BTC cell lines.

< preferred width: single column, colour in web and print >

(A) mRNA levels of G9a in BTC cell lines. (B) Expression of G9a protein and H3K9me2 in BTC cell lines. (C) Representative western blot images (cropped). (D) Correlation of G9a mRNA, G9a protein and H3K9me2 expression (Pearson). Green boxes indicate positive correlation. Abbreviations: BTC: biliary tract cancer.

### Figure 5. Cytotoxic effects of G9a inhibition in BTC cells.

< preferred width: double column, colour in web and print >

Treatment of BTC cells with G9a inhibitors BIX01294 (A), BRD4770 (B) and UNC0642 (C) over 72 hours using a serial dilution series (range 0.1-50  $\mu\text{M}$ ). (D)  $\text{IC}_{50}$  value for each G9a inhibitor and cell line. (E) Correlation (Pearson) of G9a mRNA expression, G9a protein levels, BIX01294  $\text{IC}_{50}$ , BRD4770  $\text{IC}_{50}$ , and, UNC0642  $\text{IC}_{50}$ . Green boxes indicate significant or highly significant correlation, respectively. (F) Effect of various concentrations of BIX01294 (CCSW-1:  $\text{IC}_{10/50/90} = 3.0 / 4.7 / 8.0 \mu\text{M}$ , respectively and EGi-1:  $\text{IC}_{10/50/90} = 2.6 / 7.9 / 20.0 \mu\text{M}$ , respectively) on protein expression after 24 hours of incubation. (G) Representative western blot images (cropped). \* indicate significant ( $p < 0.05$ ) and \*\* indicate highly significant ( $p < 0.01$ ) results. Abbreviations: IC: inhibitory concentration, n.d.: not determinable, UTC: untreated control.



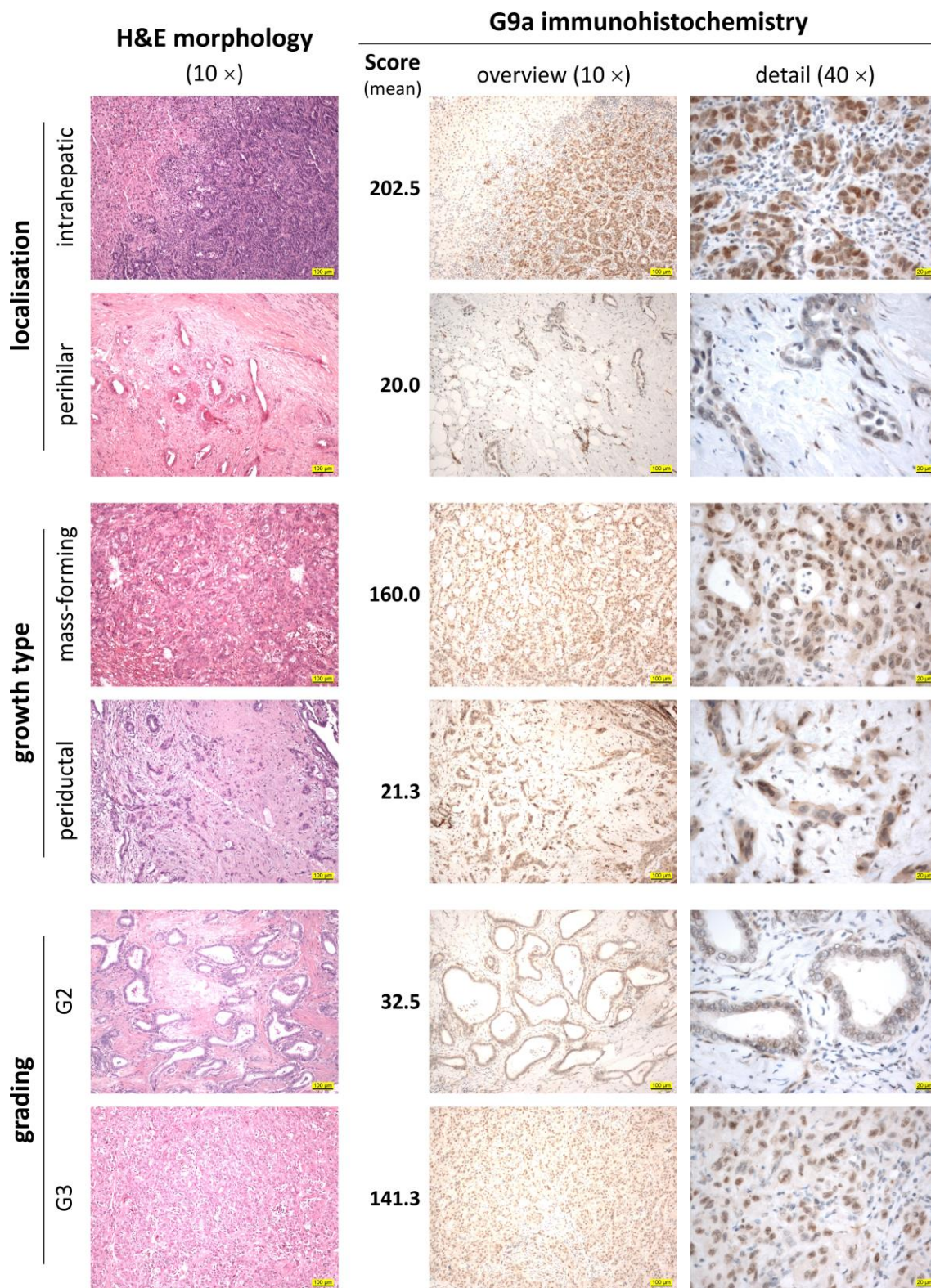


Figure 2

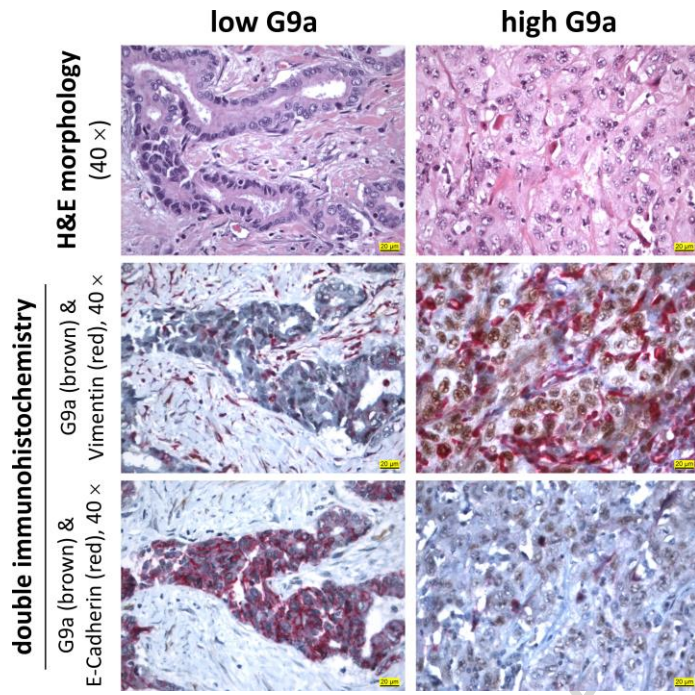


Figure 3

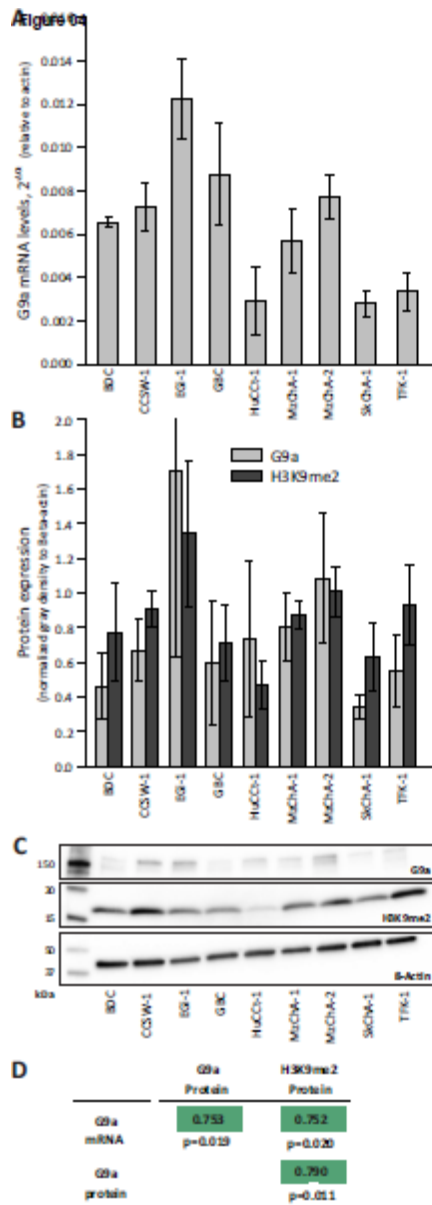


Figure 4

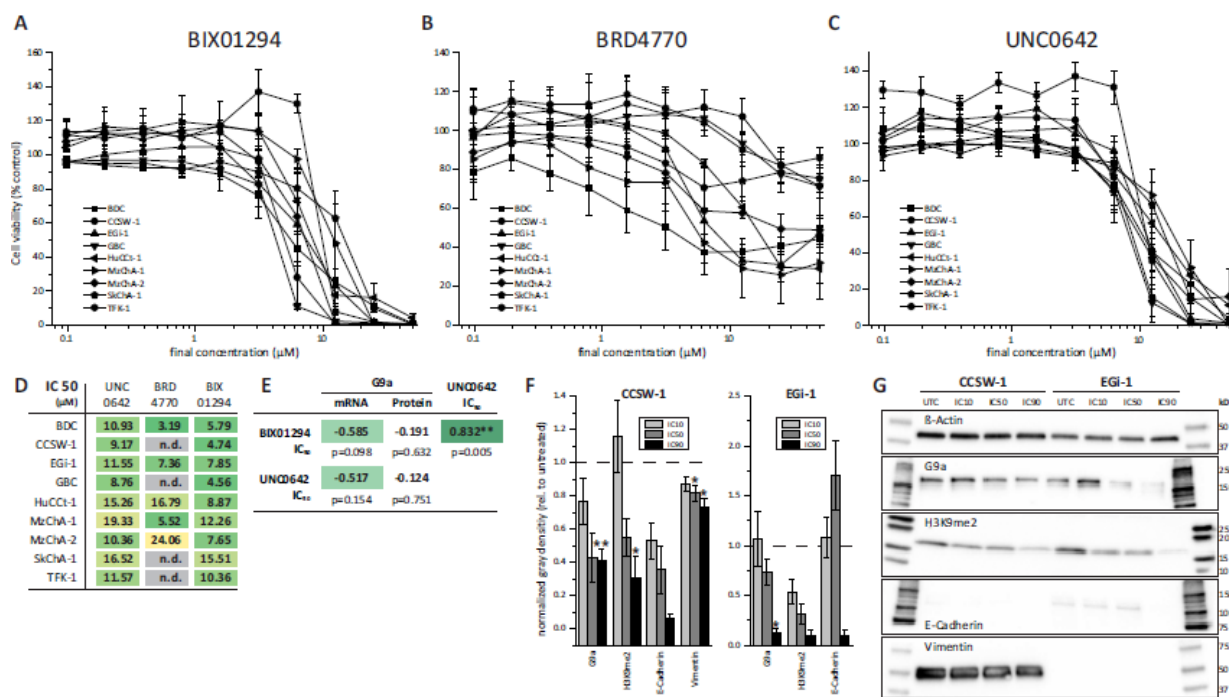


Figure 5

Title: The histone methyltransferase G9a: a new therapeutic target in biliary tract cancer

Authors: Christian MAYR et al.

Highlights:

- G9a histone methyltransferase is expressed in biliary tract cancer (BTC).
- G9a expression correlates with tumour grading, size and Vimentin expression.
- High G9a expression identifies patients with shorter survival.
- Pharmacological inhibition causes BTC cell death in vitro.